

---

# ROBUST LOCALIZATION IN WIRELESS NETWORKS FROM CORRUPTED SIGNALS

---

A PREPRINT

Muhammad Osama\*

Dave Zachariah\*

Satyam Dwivedi

Petre Stoica\*

## ABSTRACT

We address the problem of timing-based localization in wireless networks, when an unknown fraction of data is corrupted by nonideal signal conditions. While timing-based techniques enable accurate localization, they are also sensitive to such corrupted data. We develop a robust method that is applicable to a range of localization techniques, including time-of-arrival, time-difference-of-arrival and time-difference in schedule-based transmissions. The method is nonparametric and requires only an upper bound on the fraction of corrupted data, thus obviating distributional assumptions of the corrupting noise distribution. The robustness of the method is demonstrated in numerical experiments.

## 1 Introduction

Localization in wireless networks is important for applications in GPS-denied environments [2]. The next generation wireless communication systems will standardize radio signals and measurements for localization in use cases that range from mobile broadband to industrial internet-of-things networks. For accurate localization, such applications depend on techniques that use the signal time of flight between a transmitter and a receiver [1, 16].

Real-world measurements of wireless signals are prone to outliers which arise not only from sensor failures but also from signals that fail to reach the receiver in an ideal line-of-sight (LOS) manner. That is, wireless signals that may arrive at the receiver after a few reflections, diffractions or penetrations of different mediums, which we refer to as a non-line-of-sight (NLOS) situation. The real deployment of wireless technologies face repeated signal obstructions, moving objects, reflecting paths, foliage, etc. Under such non-ideal and NLOS conditions, standard measurement noise assumptions are invalid and conventional localization methods break down, as illustrated in Figure 1.

Several approaches to robust localization exist. A conservative approach is to model the NLOS effects as bounded additive measurement errors or bias [15, 17] and then estimate the node location that minimizes the worst-case error. This approach, however, can be overly conservative and sensitive to the user specified error bound. An alternative approach from the robust statistics literature is to consider the Huber contamination model [10], in which an  $\epsilon$  fraction of data samples are corrupted by a NLOS-data distribution. The NLOS distribution is either assumed to have a specific parametric form – e.g. shifted Gaussian or exponential [12, 19] in which case the positions of nodes are estimated via maximum likelihood – or is modelled nonparametrically [7, 8, 18] which is tackled using semiparametric or iterative maximum likelihood methods. An alternative approach is to apply a different, robust loss function that is insensitive to outliers [21]. While it is often assumed that the fraction of corrupted data is known, it is in practice set as an unknown user parameter.

In this paper, we propose a robust localization methodology for data obtained in the contamination setting with an unknown fraction  $\epsilon$  of NLOS data, drawing upon principles of robust risk minimization in [13]. We only assume that the user is able to set an upper bound  $\tilde{\epsilon} \geq \epsilon$ . We demonstrate the methodology in three distinct localization techniques: time-of-arrival (TOA), time-difference-of-arrival (TDOA) and time-difference in schedule-based transmissions (TDST).

---

\*Division of System and Control, Department of Information Technology, Uppsala University, Sweden. muhammad.osama@it.uu.se, dave.zachariah@it.uu.se

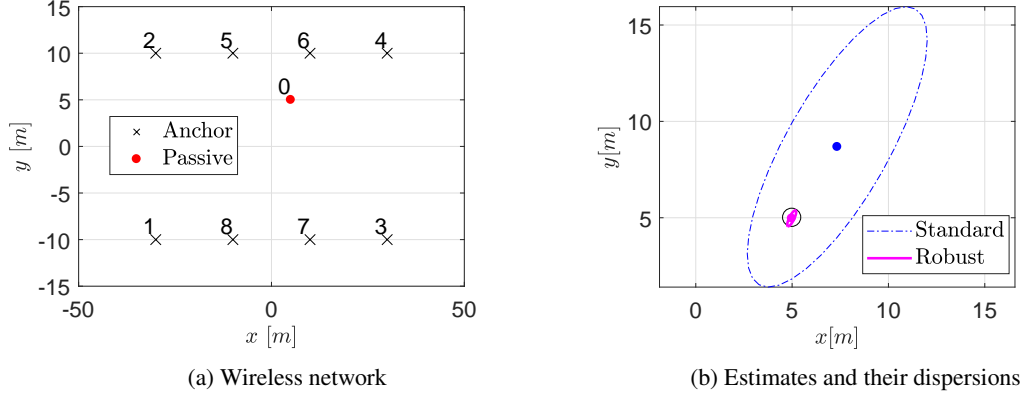


Figure 1: Self-localization of passive receiving node (o) in (a) at location (5, 5) using eight anchor nodes (x) using time-difference of arrival (TDOA). The resolution of the interarrival times are on the order of 3ns and  $n = 100$  observations are used. Here  $\epsilon = 15\%$  of the data is corrupted by non-line of sight (NLOS) outliers. • and • denote the mean position estimated using the standard nonlinear least-squares method (8) and the proposed robust method, respectively. The ellipses illustrate the dispersion of location estimates with approximately 99.9% coverage for the standard (dotted) and robust (solid) methods, respectively.

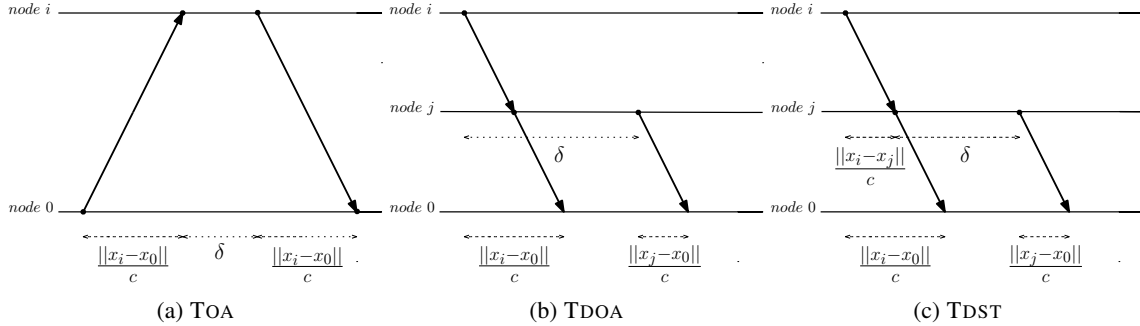


Figure 2: Timing diagrams illustrating node transmitting signals in three different localization techniques.

## 2 Problem formulation

For a general problem formulation, consider a wireless network consisting of  $N + 1$  nodes at locations

$$\{\mathbf{x}_0, \underbrace{\mathbf{x}_1, \dots, \mathbf{x}_{N_a}}_{\text{auxiliary}}, \underbrace{\mathbf{x}_{N_a+1}, \dots, \mathbf{x}_N}_{\text{anchors}}\}$$

in  $\mathbb{R}^d$  space, where only the anchor nodes have known locations. The anchors and auxiliary nodes all transmit signals that propagate through space with constant velocity. These nodes can be thought of as base stations with known and unknown locations, respectively. The signals carry signatures that enable the identification of the transmitting node.

The self-localizing node, located at  $\mathbf{x}_0$  can either be an active transceiver or a passive receiver, depending on the localization technique considered below. We let  $\theta^*$  denote set of locations of interest and our goal is to estimate this set using timing measurements at node 0. Only TDST is capable of localizing auxiliary nodes and we therefore consider  $N_a = 0$  for TOA and TDOA.

### 2.1 TOA: two-way ranging anchor nodes

In TOA, node  $\mathbf{x}_0$  is a transceiving node. At a given time, node 0 initiates a transmission to the anchor nodes. Upon receiving the signals, anchor nodes return signals, after a possible fixed delay. This leads to time-of-arrival measurements at self-localizing node 0. The TOA measurement with respect to anchor node  $i$  is then

$$\mu^{i0} = 2 \frac{\|\mathbf{x}_i - \mathbf{x}_0\|}{c} + \delta, \quad (1)$$

where  $c$  is the signal propagation velocity and  $\delta \geq 0$  is a transmission delay, see Figure 2a. The unknown location is

$$\boldsymbol{\theta}^* = \{\mathbf{x}_0\}.$$

## 2.2 TDOA: synchronous anchor nodes

In TDOA, the anchor nodes are synchronized so that they broadcast signals with respect to a common clock. Consider a pair of anchor nodes  $(i, j)$  transmitting signals. Their interarrival time at a passive self-localizing receiver node 0 is then

$$\mu^{ij} = \frac{\|\mathbf{x}_j - \mathbf{x}_0\|}{c} + \delta - \frac{\|\mathbf{x}_i - \mathbf{x}_0\|}{c}, \quad (2)$$

where  $\delta \geq 0$  is a (possible) transmission delay at node  $i$ , see Figure 2b. The unknown location is

$$\boldsymbol{\theta}^* = \{\mathbf{x}_0\}$$

## 2.3 TDST: asynchronous anchor nodes

In TDST, the anchor nodes operate asynchronously so that the transmitted signals are only coordinated through a sequence of observable signal events. Consider a pair of transeiving nodes  $(i, j)$ , such that node  $j$  transmits only *after* receiving the signal from  $j$  and a given delay. The interarrival time at the passive node is then

$$\mu^{ij} = \frac{\|\mathbf{x}_i - \mathbf{x}_j\|}{c} + \frac{\|\mathbf{x}_j - \mathbf{x}_0\|}{c} + \delta - \frac{\|\mathbf{x}_i - \mathbf{x}_0\|}{c}. \quad (3)$$

where  $\delta > 0$  is a transmission delay at node  $i$ , see Figure 2c. We allow for additional auxiliary nodes, i.e.,  $N_a \geq 0$ , so that

$$\boldsymbol{\theta}^* = \{\mathbf{x}_0, \mathbf{x}_1, \dots, \mathbf{x}_{N_a}\}$$

## 2.4 Measurements in LOS and NLOS

We let  $s \subseteq \{1, 2, \dots, N\}$  denote a set of transmitting nodes whose signals are observed by the self-localizing node at a given period. For a given  $s$ , the ideal interarrival times, from either (1), (2) or (3), can be arranged into a vector expressed as

$$\boldsymbol{\mu}(s, \boldsymbol{\theta}^*) = \frac{1}{c} \mathbf{M}(s) \boldsymbol{\rho}(\boldsymbol{\theta}^*) + \delta \mathbf{1}, \quad (4)$$

where

$$\boldsymbol{\rho}(\boldsymbol{\theta}^*) = \left[ \|\mathbf{x}_1 - \mathbf{x}_2\|, \dots, \|\mathbf{x}_N - \mathbf{x}_0\| \right]^\top,$$

is a vector of distances between all nodes,  $\mathbf{M}(s)$  is an integer matrix and  $\delta$  is a known delay parameter.

**Example 1 (TOA).** For  $N = 3$  and  $s = \{1, 2, 3\}$ , we have  $\boldsymbol{\mu}(s, \boldsymbol{\theta}^*) = [\mu^{10}, \mu^{20}, \mu^{30}]^\top$  and integer matrix

$$\mathbf{M}(s) = \begin{bmatrix} 0 & 0 & 2 & 0 & 0 & 0 \\ 0 & 0 & 0 & 0 & 2 & 0 \\ 0 & 0 & 0 & 0 & 0 & 2 \end{bmatrix}$$

When  $s$  contains at least three anchor nodes that are not coaligned,  $\boldsymbol{\theta}^*$  is uniquely determined from the set of interarrival times, see the principles of TOA in [14].

**Example 2 (TDOA).** For  $N = 3$  and  $s = \{1, 2, 3\}$ , we have  $\boldsymbol{\mu}(s, \boldsymbol{\theta}^*) = [\mu^{12}, \mu^{23}]^\top$  and integer matrix

$$\mathbf{M}(s) = \begin{bmatrix} 0 & 0 & -1 & 0 & 1 & 0 \\ 0 & 0 & 0 & 0 & -1 & 1 \end{bmatrix}$$

in (4).

When  $s$  contains at least three anchor nodes that are not coaligned,  $\boldsymbol{\theta}^*$  is uniquely determined from the set of interarrival times, see the principles of TDOA in [6].

**Example 3 (TDST).** For  $N = 3$  and  $s = \{1, 2, 3, 1\}$ , we have  $\boldsymbol{\mu}(s, \boldsymbol{\theta}^*) = [\mu^{12}, \mu^{23}, \mu^{31}]^\top$  and integer matrix

$$\mathbf{M}(s) = \begin{bmatrix} 1 & 0 & -1 & 0 & 1 & 0 \\ 0 & 0 & 0 & 1 & -1 & 1 \\ 0 & 1 & 1 & 0 & 0 & -1 \end{bmatrix}$$

in (4).

When  $s$  contains a sequence of nodes that are not all coaligned,  $\theta^*$  can be uniquely determined from the set of interarrival times, see the principles of TDST in [20, sec. 3.3] and [3, 4].

In ideal LOS conditions, a complete set is drawn as  $s \sim p_{\text{LOS}}(s)$ , where the distribution is possibly degenerate. For each completed set  $s$ , the self-localizing node obtains noisy measurements  $\mathbf{z}$  of the interarrival times  $\boldsymbol{\mu}(s, \theta^*)$ . That is,

$$\mathbf{z} \sim p_{\text{LOS}}(\mathbf{z}|s) \quad (5)$$

where the mean of  $p_{\text{LOS}}(\mathbf{z}|s)$  equals  $\boldsymbol{\mu}(s, \theta^*)$  in (4).

In practical wireless environments, however, the pair  $(s, \mathbf{z})$  is not always observed in the ideal condition described above but rather drawn from

$$p(s, \mathbf{z}) = (1 - \epsilon) p_{\text{LOS}}(s, \mathbf{z}) + \epsilon p_{\text{NLOS}}(s, \mathbf{z}), \quad (6)$$

where  $p_{\text{NLOS}}(s, \mathbf{z})$  is an unknown corrupting distribution, that generates outlier noise and biases such that the mean of  $p_{\text{NLOS}}(\mathbf{z}|s)$  may not equal  $\boldsymbol{\mu}(s, \theta^*)$  [10, 21], and  $\epsilon$  is an unknown fraction of corrupted data.

The problem then is to estimate  $\theta^*$  given data  $\{(s_1, \mathbf{z}_1), \dots, (s_n, \mathbf{z}_n)\}$  drawn i.i.d. from (6). We assume only that the quality of the data can be specified by an upper bound  $\tilde{\epsilon} \geq \epsilon$  [9, ch. 1].

### 3 Method

Let the parameter  $\theta$  represent the unknown locations  $\theta^*$ . Assuming a set of anchor locations and transmission sequences that yields identifiable locations, we have that

$$\theta^* \equiv \arg \min_{\theta} \mathbb{E} \left[ \|\mathbf{z} - \boldsymbol{\mu}(s, \theta)\|^2 \right], \quad (7)$$

with respect to the unknown distribution  $p_{\text{LOS}}(s, \mathbf{z})$ . Note that the right-hand side of (7) assumes that  $\mathbf{z}$  has finite second-order moments. The standard estimator of  $\theta^*$  is the nonlinear least-squares method,

$$\hat{\theta} = \arg \min_{\theta} \frac{1}{n} \sum_{i=1}^n \|\mathbf{z}_i - \boldsymbol{\mu}(s_i, \theta)\|^2, \quad (8)$$

where  $(s_i, \mathbf{z}_i) \sim p(s, \mathbf{z})$  in (6). Under standard regularity conditions  $\hat{\theta}$  is asymptotically consistent, and corresponds to the maximum likelihood estimate under white Gaussian noise, when  $\epsilon = 0$  [11]. For  $\epsilon > 0$ , however,  $\hat{\theta}$  is not robust to corrupted samples that arise in NLOS conditions, as described by (6).

#### 3.1 Robust localization

We now propose a robust method which automatically identifies corrupted samples and assigns them low weight while jointly estimating  $\theta^*$ .

Consider the following fitting criterion

$$\mathbb{E}_{\boldsymbol{\pi}} \left[ \|\mathbf{z} - \boldsymbol{\mu}(s, \theta)\|^2 \right], \quad (9)$$

where, in lieu of  $p_{\text{LOS}}(s, \mathbf{z})$  in (7), we use a nonparametric distribution

$$p(s, \mathbf{z}; \boldsymbol{\pi}) = \sum_{i=1}^n \pi_i \delta(s - s_i, \mathbf{z} - \mathbf{z}_i), \quad (10)$$

with probability weights  $\boldsymbol{\pi}$  that belong to the set

$$\Pi = \{\boldsymbol{\pi} \geq \mathbf{0} : \mathbf{1}^\top \boldsymbol{\pi} = 1\}$$

We denote the entropy of the distribution  $p(s, \mathbf{z}; \boldsymbol{\pi})$  as

$$\mathbb{H}(\boldsymbol{\pi}) \triangleq - \sum_{i=1}^n \pi_i \ln \pi_i \geq 0 \quad (11)$$

It can then be seen that the standard method (8) corresponds to minimizing (9) using the empirical distribution  $p(s, \mathbf{z}; n^{-1}\mathbf{1})$ , which attains a maximum entropy of  $\ln n$ . Given the bound  $\tilde{\epsilon} \geq \epsilon$ , we expect at least  $(1 - \tilde{\epsilon})n$  uncorrupted samples and that the support of  $p(s, \mathbf{z}; \boldsymbol{\pi})$  should cover them. In this case, its maximum entropy would

equal  $\ln[(1 - \tilde{\epsilon})n]$  and the search over the unknown support turns (9) into the following joint optimization problem

$$\begin{aligned} \min_{\boldsymbol{\theta}, \boldsymbol{\pi} \in \Pi} \quad & \sum_{i=1}^n \pi_i \|z_i - \boldsymbol{\mu}(s_i, \boldsymbol{\theta})\|^2 \\ \text{subject to} \quad & \mathbb{H}(\boldsymbol{\pi}) \geq \ln[(1 - \tilde{\epsilon})n]. \end{aligned} \quad (12)$$

Intuitively, the above minimization problem estimates  $\boldsymbol{\theta}$  while assigning weights  $\pi_i$  to each point such that the overall weighted squared-error loss is minimized. Smaller weights are assigned to datapoints which are corrupted due to NLOS and larger weights are assigned to uncorrupted points, see [13] for a general description of the approach. In this way, (12) enables robust localization of the auxiliary and receiver nodes. In the next subsection, we give a blockwise algorithm for solving (12).

### 3.2 Blockwise minimization algorithm

For a fixed  $\tilde{\boldsymbol{\theta}}$ , define

$$\hat{\boldsymbol{\pi}}(\tilde{\boldsymbol{\theta}}) = \begin{cases} \arg \min_{\boldsymbol{\pi} \in \Pi} \sum_{i=1}^n \pi_i \ell_{\tilde{\boldsymbol{\theta}}}(s_i, z_i), \\ \text{s.t. } \mathbb{H}(\boldsymbol{\pi}) \geq \ln[(1 - \tilde{\epsilon})n] \end{cases} \quad (13)$$

and, similarly, for a fixed  $\tilde{\boldsymbol{\pi}}$ , define

$$\hat{\boldsymbol{\theta}}(\tilde{\boldsymbol{\pi}}) = \arg \min_{\boldsymbol{\theta}} \sum_{i=1}^n \tilde{\pi}_i \ell_{\boldsymbol{\theta}}(s_i, z_i). \quad (14)$$

Together (13) and (14) form a blockwise coordinate descend algorithm which we summarize in Algorithm 1, that is guaranteed to converge to a critical point of (12) under fairly general conditions [5]. The weighted nonlinear least-squares problem in (14) is readily solved using any numerical search technique, while (13) requires solving a convex problem, and can be computed with a barrier method that is much more efficient than general purpose numerical packages such as *cvx*.

---

#### Algorithm 1 Robust Localization

---

- 1: Input:  $\{(s_i, z_i)\}_{i=1}^n, \tilde{\epsilon}$  and  $\boldsymbol{\pi}^{(0)} = n^{-1}\mathbf{1}$
  - 2: Set  $k := 0$
  - 3: **repeat**
  - 4:  $\boldsymbol{\theta}^{(k+1)} = \hat{\boldsymbol{\theta}}(\boldsymbol{\pi}^{(k)})$
  - 5:  $\boldsymbol{\pi}^{(k+1)} = \hat{\boldsymbol{\pi}}(\boldsymbol{\theta}^{(k+1)})$
  - 6:  $k := k + 1$
  - 7: **until convergence**
  - 8: Output:  $\hat{\boldsymbol{\theta}} = \boldsymbol{\theta}^{(k)}, \hat{\boldsymbol{\pi}} = \boldsymbol{\pi}^{(k)}$
- 

## 4 Experimental results

In this section, we illustrate the wide applicability of the proposed robust localization method using synthetic TOA, TDOA and TDST data, respectively. The performance is evaluated using the localization error

$$\Delta(\hat{\boldsymbol{x}}) = \|\boldsymbol{x} - \hat{\boldsymbol{x}}\|_2$$

where  $\boldsymbol{x}$  is the node location of interest.

We observe  $n = 100$  measurements from

$$p(s, \boldsymbol{z}) = (1 - \epsilon) p_{\text{LOS}}(s, \boldsymbol{z}) + \epsilon p_{\text{NLOS}}(s, \boldsymbol{z}). \quad (15)$$

The LOS distribution is

$$p_{\text{LOS}}(s, \boldsymbol{z}) = \underbrace{\mathcal{N}(\boldsymbol{\mu}(s, \boldsymbol{\theta}^*), \sigma_{\text{LOS}}^2 \mathbf{Q})}_{p_{\text{LOS}}(\boldsymbol{z}|s)} \underbrace{\mathcal{U}(s)}_{p_{\text{LOS}}(s)}, \quad (16)$$

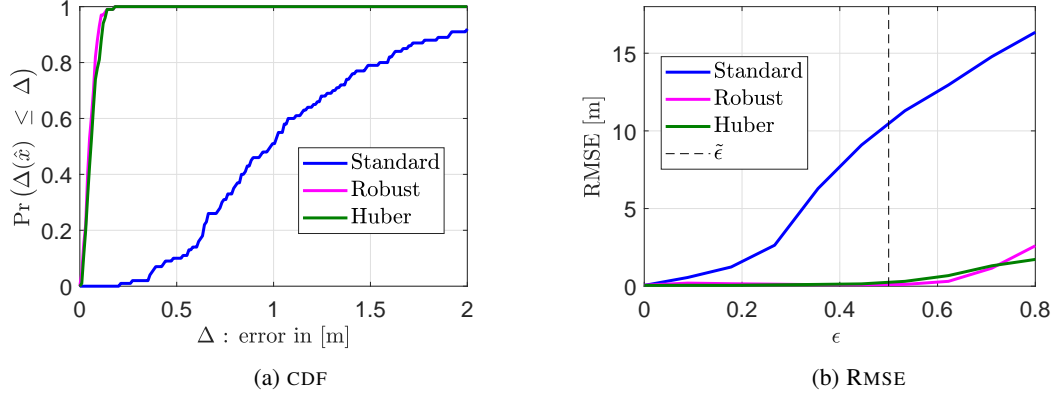


Figure 3: Performance and sensitivity in TOA. (a) Cumulative distribution functions of localization errors  $\Delta(\hat{\mathbf{x}})$  of target node in Figure 1a using 100 Monte Carlo runs. Unknown corruption fraction was  $\epsilon = 15\%$  and the upper bound used in the robust method was set to  $\tilde{\epsilon} = 20\%$ . (b) Root-mean square error in [m] as a function of  $\epsilon$  for the target node using standard, robust and Huber methods. Results based on 50 Monte Carlo simulations. For the proposed robust method the upper bound was  $\tilde{\epsilon} = 50\%$ .

where adjacent timing measurement errors have correlation structure given by  $\mathbf{Q}$ . The uniform distribution  $\mathcal{U}(s)$  draws  $s$  from a set  $\mathcal{S}$ . The corrupting NLOS distribution is

$$p_{\text{NLOS}}(s, \mathbf{z}) = \underbrace{\mathcal{E}(\boldsymbol{\mu}(s, \boldsymbol{\theta}^*) + \mu_{\text{NLOS}})}_{p_{\text{NLOS}}(\mathbf{z}|s)} \underbrace{\mathcal{U}(s)}_{p_{\text{NLOS}}(s)}. \quad (17)$$

where we consider an exponential distribution with measurement bias  $\mu_{\text{NLOS}}$ . We set  $\sigma_{\text{LOS}} = 3$  ns and the corrupted signal bias  $\mu_{\text{NLOS}} = 75$  ns. Unless otherwise specified, the unknown corruption fraction is set to  $\epsilon = 15\%$ .

*Remark:* The code for the experiments is available at github.

#### 4.1 TOA: two-way ranging anchor nodes

Consider a wireless network consisting of  $N = 8$  nodes as shown in Figure 1a. Since the TOA measurements are uncorrelated,  $\mathbf{Q}$  in (16) is a diagonal matrix. The unknown location of interest is

$$\boldsymbol{\theta}^* = \{\mathbf{x}_0\} = \{[5, 5]^\top\}.$$

The sequence set  $\mathcal{S}$  consists of two sequences  $s_0 = \{6, 5, 7, 8\}$  and  $s_1 = \{4, 3, 2, 1\}$  where the node numbers are given in Figure 1a. The sequences have been selected so that the anchor nodes are not coaligned in either  $s_0$  or  $s_1$ .

In the case of TOA, the measurement model (1) admits an (overparameterized) linear form which is ideal for classical methods in robust statistics, such as the Huber method [21]. The Huber method is thus tailored for the task of TOA and therefore provides a useful benchmark. We compare it to the standard nonlinear least-squares method (8) and the proposed method (12).

Figure 3a shows the cumulative distribution functions (CDF) of the localization error  $\Delta(\hat{\mathbf{x}})$  over 100 Monte Carlo simulations, setting  $\tilde{\epsilon} = 20\%$  in Algorithm 1. As expected there is a severe performance degradation of the standard method with corrupted signals. To investigate the sensitivity of the results with respect to the unknown corruption fraction, we also plot the root-mean-square error (RMSE), i.e.  $\sqrt{\mathbb{E}[\Delta^2(\hat{\mathbf{x}})]}$ , versus  $\epsilon$  for all three methods. For the proposed method we set a very conservative upper bound  $\tilde{\epsilon} = 50\%$  in Algorithm 1. Figure 3b shows the RMSE for the different methods, where we see that the robust method is insensitive to  $\epsilon$ , with a graceful rise in RMSE when  $\epsilon$  exceeds  $\tilde{\epsilon}$ . In sum, the proposed method outperforms the standard nonlinear least-squares method and is close to the benchmark provided by the TOA-tailored Huber method.

The results are corroborated also in Figure 4 which compare RMSE as a function of  $x_0$ . It can be seen that the robust method is more sensitive towards the edges of the vertical boundaries than the benchmark.

#### 4.2 TDOA: synchronous anchor nodes

We consider again the network in Figure 1a, but now the self-localizing node is a passive receiver. Since TDOA measurements are correlated, we set  $\mathbf{Q}$  with 1s along the diagonal and  $\frac{1}{3}$  along the off-diagonal entries. The unknown

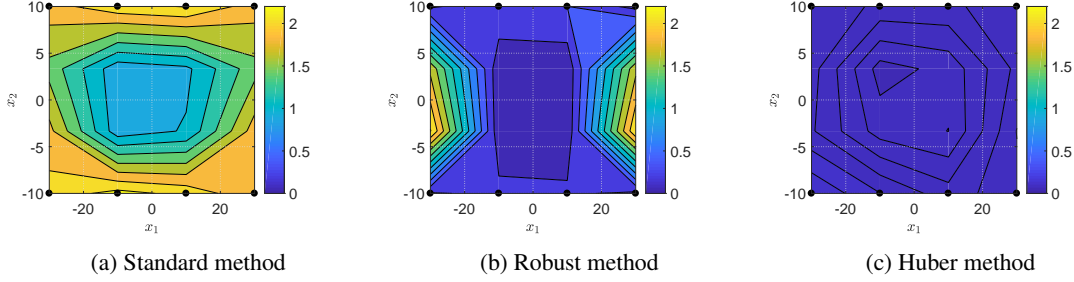


Figure 4: Performance in TOA across space. Root-mean square error in [m] with respect to different locations  $\mathbf{x}_0$ . Results based on 50 Monte Carlo runs.

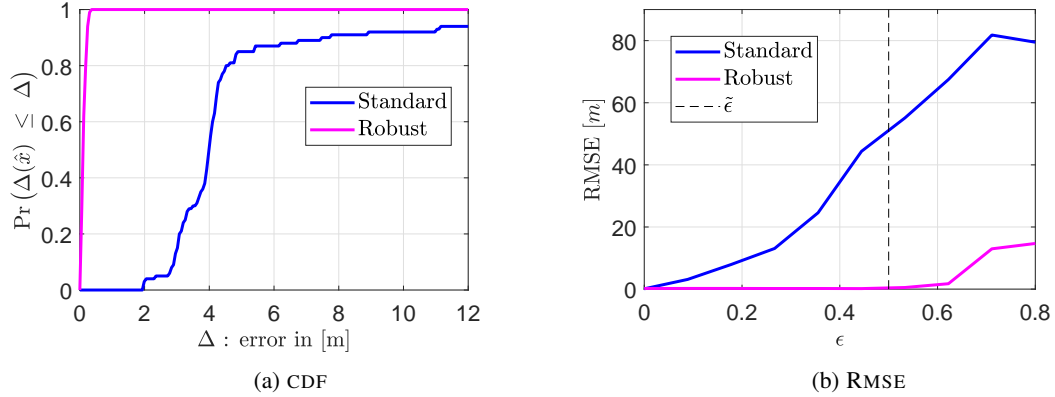


Figure 5: Performance and sensitivity in TDOA. (a) Cumulative distribution functions of localization errors  $\Delta(\hat{\mathbf{x}})$  of target node in Figure 1a using 100 Monte Carlo runs. Unknown corruption fraction was  $\epsilon = 15\%$  and the upper bound used in the robust method was set to  $\tilde{\epsilon} = 20\%$ . (b) Root-mean square error in [m] as a function of  $\epsilon$  for the target node using standard and robust methods. Results based on 50 Monte Carlo simulations. For the proposed robust method the upper bound was  $\tilde{\epsilon} = 50\%$ .

location of interest is

$$\boldsymbol{\theta}^* = \{\mathbf{x}_0\} = \{[5, 5]^\top\}.$$

As in the case of TOA above, we use the sequence set  $\mathcal{S}$  with  $s_0 = \{6, 5, 7, 8\}$  and  $s_1 = \{4, 3, 2, 1\}$ .

Note that the measurement model (2) does not admit a linear re-parametrization and therefore the Huber method is not readily applicable for TDOA. We therefore compare only the standard nonlinear least-squares method (8) and the proposed method (12).

Figure 5a shows CDFs of the localization error  $\Delta(\hat{\mathbf{x}})$  over 100 Monte Carlo simulations, setting  $\tilde{\epsilon} = 20\%$  in Algorithm 1. The performance characteristics are similar to those in Figure 3a, but the absolute error levels are not directly comparable due to different measurement setups. The sensitivity respect to the unknown corruption fraction  $\epsilon$  is also shown in 5b using RMSE versus  $\epsilon$  for both methods. We use a very conservative upper bound  $\tilde{\epsilon} = 50\%$  in Algorithm 1. The proposed method is consistently robust and insensitive to corrupted data in contrast to the standard method for which the errors rise drastically with  $\epsilon$ . Figure 4 shows that the robust method yields substantial error reduction across space.

Finally, we illustrate the ability of the proposed method to effectively isolate corrupted NLOS samples. Since the data is generated synthetically we can classify each sample from  $p_{\text{NLOS}}(\mathbf{z}|s)$  as ‘corrupted’, denoted  $\mathcal{C}(\mathbf{z}) = 1$ . The method solves (12) and learns probability weights  $\hat{\boldsymbol{\pi}}$  for which corrupted measurements are assigned low weights. If a weight is below a certain threshold, we may classify the corresponding sample  $\mathbf{z}$  as an outlier, denoted  $\hat{\mathcal{C}}(\mathbf{z}) = 1$ . We set the weight threshold to  $10^{-5}$  and assess the resulting probability of correct detection  $\Pr\{\hat{\mathcal{C}}(\mathbf{z}) = 1|\mathcal{C}(\mathbf{z}) = 1\}$  as well as the probability of false alarm  $\Pr\{\hat{\mathcal{C}}(\mathbf{z}) = 1|\mathcal{C}(\mathbf{z}) = 0\}$  in Figure 7a. We fix the upper bound  $\tilde{\epsilon} = 50\%$  and vary the unknown fraction  $\epsilon$ , using 50 Monte Carlo runs. It can be seen that the proposed method can effectively isolate NLOS samples with a low false-alarm rate.

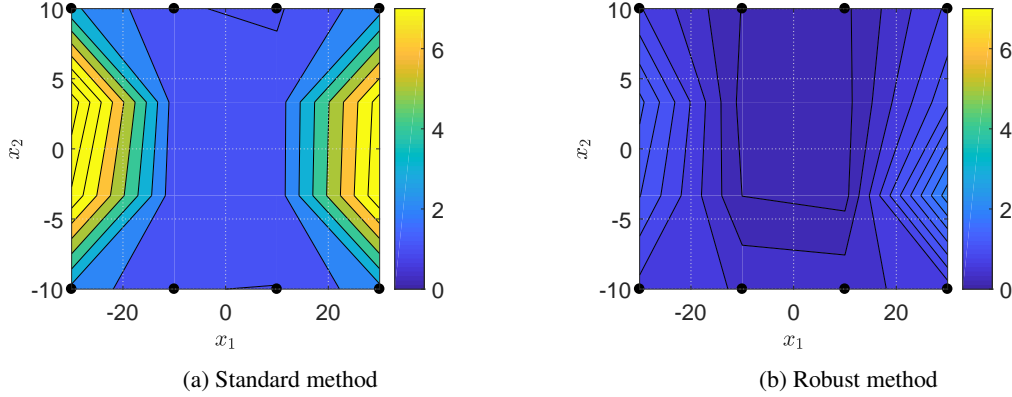


Figure 6: Performance in TDOA across space. Root-mean square error in [m] with respect to different locations  $\mathbf{x}_0$ . Results based on 50 Monte Carlo runs.

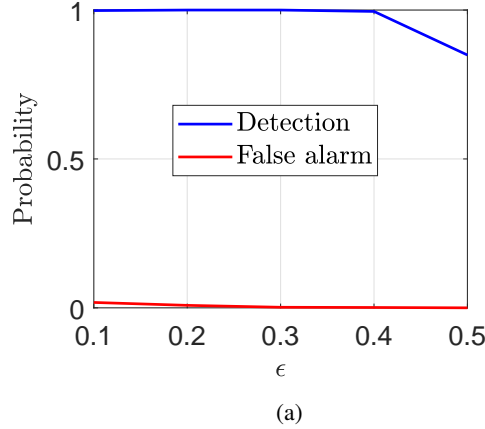


Figure 7: The weights in robust method can be used to classify samples  $\mathcal{C}(z) \in \{0, 1\}$  as ‘normal’ or ‘corrupted’. This yields corresponding probabilities of correct detection  $\Pr\{\hat{\mathcal{C}}(z) = 1 | \mathcal{C}(z) = 1\}$  and false alarm  $\Pr\{\hat{\mathcal{C}}(z) = 1 | \mathcal{C}(z) = 0\}$  at a fixed upper bound  $\tilde{\epsilon} = 50\%$ .

### 4.3 TDST: asynchronous anchor nodes

We consider the network in Figure 1a, but now the self-localizing node is a passive receiver and the anchor nodes are asynchronous. Since TDST measurements are correlated, we set  $\mathbf{Q}$  with 1s along the diagonal and  $\frac{1}{3}$  along the off-diagonal entries. The unknown location of interest is

$$\boldsymbol{\theta}^* = \{\mathbf{x}_0\} = \{[5, 5]^\top\}.$$

We use sequence set  $\mathcal{S}$  that consists of four sequences:  $s_0 = \{6, 4, 5, 3\}$ ,  $s_1 = \{3, 6, 4, 5\}$ ,  $s_2 = \{5, 3, 6, 4\}$  and  $s_3 = \{4, 5, 3, 6\}$ , following the scheme described in [4].

As in TDOA, the Huber method is not readily applicable for TDST. We therefore compare only the standard nonlinear least-squares method (8) and the proposed method (12).

Figure 8a shows CDFs of the localization error  $\Delta(\hat{\mathbf{x}})$ . The characteristics are similar to those in Figure 3a. The sensitivity with respect to the unknown corruption fraction  $\epsilon$  is also shown in 8b using RMSE versus  $\epsilon$  along with a very conservative upper bound  $\tilde{\epsilon} = 50\%$  in Algorithm 1. In sum, the proposed method also robustifies self-localization in TDST.

Finally, we consider a more challenging wireless network configuration, where one anchor node is replaced by an auxiliary node ( $N_a = 1$ ) at an unknown location as shown in Figure 9a. Thus we demonstrate the ability to passively localize auxiliary nodes using asynchronous anchor nodes [3, 4, 20] in adverse NLOS conditions. The locations of



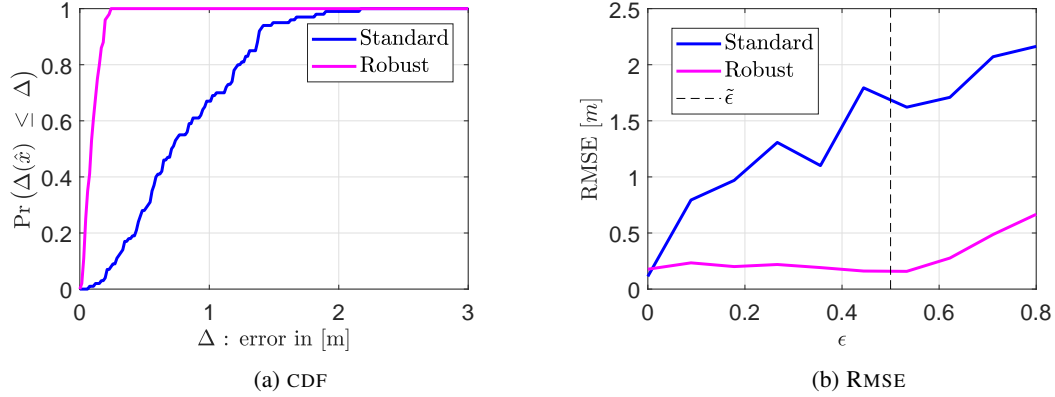


Figure 8: Performance and sensitivity in TDST. (a) Cumulative distribution functions of localization errors  $\Delta(\hat{x})$  of target node in Figure 1a using 100 Monte Carlo runs. Unknown corruption fraction was  $\epsilon = 15\%$  and the upper bound used in the robust method was set to  $\tilde{\epsilon} = 20\%$ . (b) Root-mean square error in [m] as a function of  $\epsilon$  for the target node using standard and robust methods. Results based on 50 Monte Carlo simulations. For the proposed robust method the upper bound was  $\tilde{\epsilon} = 50\%$ .

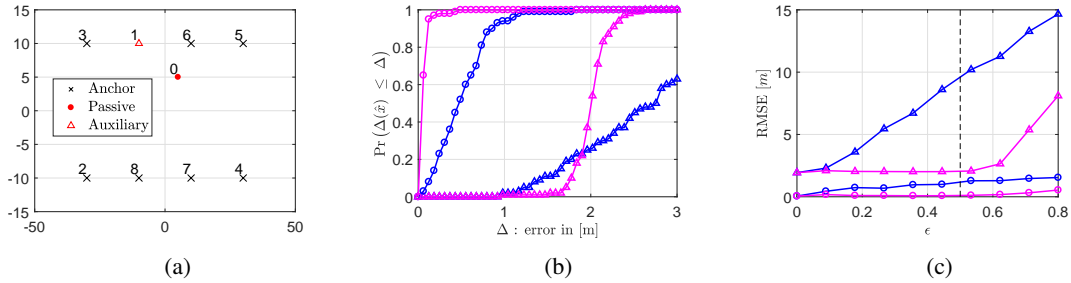


Figure 9: Performance and sensitivity in TDST when localizing additional auxiliary node. (a) Configuration of wireless network. (b) CDF of localization errors  $\Delta(\hat{x})$  using 100 Monte Carlo runs for auxiliary (triangle) and passive node (circle), using the standard (blue) and robust (magenta) methods, respectively. Unknown corruption fraction is  $\epsilon = 15\%$ . (c) Root mean square error (RMSE)  $\sqrt{\mathbb{E}[\Delta^2(\hat{x})]}$  as a function of fraction of corrupted data  $\epsilon$  using standard (blue) and robust (magenta) method, for passive (circles) and auxiliary (triangles) nodes, respectively. Results based on 50 Monte Carlo simulations  $\tilde{\epsilon} = 50\%$  indicated by the black-dashed line.

interest are

$$\theta^* = \{\mathbf{x}_0, \mathbf{x}_1\} = \{[5, 5]^\top, [-10, 10]^\top\}.$$

We use the sequence set  $\mathcal{S} = \{s_0, s_1\}$ , where  $s_0 = \{2, 3, 4, 5, 6, 7, 8, 2, 3, 4, 5, 6, 7, 8\}$  and  $s_1 = \{2, 1, 3, 1, 4, 1, 5, 1, 6, 1, 7, 1, 8, 1\}$ . The first sequence set  $s_0$  involves only the anchor nodes and ensures that the passive node location is identifiable. The second sequence  $s_1$  ensures that the auxiliary node location is identifiable, see [20].

Figure 9b summarizes the distribution of localization errors  $\Delta(\hat{x})$  for the passive and auxiliary nodes, respectively. Note that auxiliary node is a harder problem that involves two unknown locations  $\mathbf{x}_0$  and  $\mathbf{x}_1$ . The difficulty is compounded in the NLOS scenario when timing measurements for  $s_1$  are corrupted. In Figure 9c we see that the localization performance degrades very rapidly under NLOS conditions using the standard method, whereas the proposed method is resilient.

## 5 Conclusion

We have developed a robust method for localization of nodes in wireless networks using timing-based measurements. The method is applicable to a wide range of localization technologies. Its robustness properties against data corrupted due to non-ideal and non-line-of-sight signal conditions are demonstrated using three different configurations: TOA,

TDOA and TDST. The proposed method does not make any assumptions on the form of corrupting noise distribution, and uses only an upper bound on the fraction of corrupted data.

## References

- [1] Amir Beck, Petre Stoica, and Jian Li. Exact and approximate solutions of source localization problems. *IEEE Transactions on signal processing*, 56(5):1770–1778, 2008.
- [2] James J Caffery and Gordon L Stuber. Overview of radiolocation in cdma cellular systems. *IEEE Communications Magazine*, 36(4):38–45, 1998.
- [3] Baptiste Cavarec, Satyam Dwivedi, Mats Bengtsson, and Peter Händel. Schedule based self localization of asynchronous wireless nodes with experimental validation. In *2017 IEEE International Conference on Acoustics, Speech and Signal Processing (ICASSP)*, pages 5975–5979. IEEE, 2017.
- [4] Satyam Dwivedi, Alessio De Angelis, and Peter Händel. Scheduled uwb pulse transmissions for cooperative localization. In *2012 IEEE International Conference on Ultra-Wideband*, pages 6–10. IEEE, 2012.
- [5] Luigi Grippo and Marco Sciandrone. On the convergence of the block nonlinear gauss–seidel method under convex constraints. *Operations research letters*, 26(3):127–136, 2000.
- [6] Fredrik Gustafsson and Fredrik Gunnarsson. Positioning using time-difference of arrival measurements. In *2003 IEEE International Conference on Acoustics, Speech, and Signal Processing, 2003. Proceedings.(ICASSP'03).*, volume 6, pages VI–553. IEEE, 2003.
- [7] Ulrich Hammes, Eric Wolsztynski, and Abdelhak M Zoubir. Semi-parametric geolocation estimation in nlos environments. In *2008 16th European Signal Processing Conference*, pages 1–5. IEEE, 2008.
- [8] Ulrich Hammes, Eric Wolsztynski, and Abdelhak M Zoubir. Robust tracking and geolocation for wireless networks in nlos environments. *IEEE Journal of Selected Topics in Signal Processing*, 3(5):889–901, 2009.
- [9] Frank R Hampel, Elvezio M Ronchetti, Peter J Rousseeuw, and Werner A Stahel. *Robust statistics: the approach based on influence functions*, volume 196. John Wiley & Sons, 2011.
- [10] Peter J Huber. *Robust statistics*. Springer, 2011.
- [11] S.M. Kay. *Fundamentals of Statistical Signal Processing, Vol. I—Estimation theory*. Prentice Hall, 1993.
- [12] Michael McGuire, Konstantinos N Plataniotis, and Anastasios N Venetsanopoulos. Data fusion of power and time measurements for mobile terminal location. *IEEE Transactions on Mobile Computing*, 4(2):142–153, 2005.
- [13] Muhammad Osama, Dave Zachariah, and Peter Stoica. Robust risk minimization for statistical learning. *arXiv:1910.01544*, 2019.
- [14] S Ravindra and SN Jagadeesha. Time of arrival based localization in wireless sensor networks: A linear approach. *arXiv preprint arXiv:1403.6697*, 2014.
- [15] Xiufang Shi, Brian DO Anderson, Guoqiang Mao, Zaiyue Yang, Jiming Chen, and Zihuai Lin. Robust localization using time difference of arrivals. *IEEE Signal Processing Letters*, 23(10):1320–1324, 2016.
- [16] Petre Stoica and Jian Li. Lecture notes-source localization from range-difference measurements. *IEEE Signal Processing Magazine*, 23(6):63–66, 2006.
- [17] Slavisa Tomic, Marko Beko, Rui Dinis, and Paulo Montezuma. A robust bisection-based estimator for toa-based target localization in nlos environments. *IEEE Communications Letters*, 21(11):2488–2491, 2017.
- [18] Feng Yin, Carsten Fritsche, Fredrik Gustafsson, and Abdelhak M Zoubir. Toa-based robust wireless geolocation and cramer-rao lower bound analysis in harsh los/nlos environments. *IEEE transactions on signal processing*, 61(9):2243–2255, 2013.
- [19] Feng Yin, Abdelhak M Zoubir, Carsten Fritsche, and Fredrik Gustafsson. Robust cooperative sensor network localization via the em criterion in los/nlos environments. In *2013 IEEE 14th Workshop on Signal Processing Advances in Wireless Communications (SPAWC)*, pages 505–509. IEEE, 2013.
- [20] Dave Zachariah, Alessio De Angelis, Satyam Dwivedi, and Peter Händel. Schedule-based sequential localization in asynchronous wireless networks. *EURASIP Journal on Advances in Signal Processing*, 2014(1):16, 2014.
- [21] Abdelhak M Zoubir, Visa Koivunen, Esa Ollila, and Michael Muma. *Robust statistics for signal processing*. Cambridge University Press, 2018.